International Journal of Engineering & Technology, 7 (4.31) (2018) 214-219

International Journal of Engineering & Technology

Website: www.sciencepubco.com/index.php/IJET

Research paper



A Two Dimensional Facial Features Analysis for Gender-based Comparison Using Morphometrics Approach

Olalekan Agbolade[1*], Azree Shahrel Ahmad Nazri[2]

Faculty of Computer Science & Information Technology,
Universiti Putra Malaysia, Serdang, Selangor, Malaysia
**Corresponding author E-mail: lokoprof@yahoo.com*

Abstract

Making a gender comparison between male and female is not a difficult task for human beings but the science of gender comparison of faces by humans is completely unfathomable due to commonality of gender comparison in both humans and other animal species. Significant gender differences between masculine and feminine exist in many facial regions such as eyes, nose, mouth, cheek and chin; which have not been critically looked into. This research characterizes and analyzes the gender comparison in the human face as a function of face features and identifies the features which contribute significantly to the uniqueness of the face using morphometrics techniques such as Principal Component Analysis (PCA), Thin-Plate Spline (TPS) Warping and Procrustes Superimposition (PS). The results demonstrate that the male face is significantly different from that of female based on the analysis of the selected facial features which provides the basis for gender-based comparison of faces.

Keywords: *Gender Comparison; Procrustes Superimposition; PCA; Sexual Dimorphism; TPS*

1. Introduction

Gender comparison in cognitive abilities is a hot topic especially the proposed reasons for the findings. Over the decades, researchers have been looking for a way to compare gender-based human faces but due to the complexity of the human facial features, efforts to critically analyze the facial features in both masculine and feminine have not been yielding expected result especially with the application of morphometrics compared with face recognition and facial expression in computer vision. However, the significance of this study is that the method is completely race dependent and not machine dependent as each race has its own unique facial features that distinguish him/her from other race.

By using the anatomical reference points, Geometric Morphometrics techniques are widely used by researchers to descript faces in a different area of computer vision such as face recognition, face detection, facial expression recognition, the study of changes in facial morphology due to growth, or gender comparison. But all researchers would agree that facial gender-based comparison and facial recognition share some conceptual processes, especially in architecture, which portrays a step-by-step configuration of processing blocks that is compliant with a pattern of classical recognition model as shown in Figure 1.

2. Literature Review

Gender-based Comparison represents a group of morphological characteristics in form of shape and size that differentiate masculine from feminine. There have been a handful of researches on gender-based classification by comparing facial features. Tanikawa, et al. [1] demonstrated a gender comparison in the facial surface of adult humans using discriminant function analysis (DFA) for sex determination by extracting 185 variables describing facial surface configuration features and comparing using t-tests. The facial surface morphology was examined by wire mesh fitting on each face. The reports showed significance between the group of 16 out of 185 variables; the wire mesh fitting results showed that the forehead, chin and eyes were in vertically lower positions in the male group than in the female group. The nose and cheek were more protuberant in the male group than the female group. A combination partial least-squares regression (PLSR) with bootstrapped response-based imputation modeling (BRIM) was proposed by Matthews, et al. [2] to test gender classification in the craniofacial shape of 1-year-old babes by observing the differences in the nose and a recession of the forehead in boys relative to that of the girls. The results suggested that the level of dimorphic trait expression of individual is continuous in the population. Variations in face shape and form were evaluated by Koudelová, et al. [3] using Discriminant Component Analysis (DCA) and Principal Component Analysis (PCA) in geometric morphometrics to compare the differences between the average boys and girls faces from 12 to 15 years in facial scans from healthy Caucasian children where the average faces were superimposed and color-coded maps were used to evaluate changes. The reports show no significant gender difference in shape in any age category and also no differences in form between the age of 12 and 13 years but from age 14, there is a slight separation which was statistical. The reports concluded that generally, males had more prominent deeply set eyes, eyebrow ridges, flatter cheek area, and a more prominent chin area and nose. Ferrario, et al. [4] proposed a method of Euclidean Distance Matrix Analysis (EDMA) to point out the differences between shape and size by computing all possible linear distances between pairs of 22 facial landmarks. The reports showed that the face was narrower and shorter in women than in

Copyright © 2018 Agbolade & Nazri. This is an open access article distributed under the Creative Commons Attribution License, which permits unrestricted use, distribution, and reproduction in any medium, provided the original work is properly cited.

men, with a global shape demonstration difference proving that the female face is squarer than the male face and the male face is more rectangular than the female face. DeLacoste-Utamsing and Holloway [5] suggested a sex difference in the shape and surface area of the human corpus callosum. The gender comparison was striking in the splenium, the posterior portion or the caudal. The male splenium is both less bulbous and smaller than the female counterpart showing gender differences. Little, et al. [6] showed in their work that measurements of symmetry and sexual dimorphism from faces are related in humans, both in Europeans and African hunter-gatherers and in a non-human primate. Scott, et al. [7] classified gender differences using the method of an ancestral signal of heritable mate value and reported twelve populations with a very various levels of economic development with a perceptions that masculine males look strongly aggressive with development and specifically, urbanization.

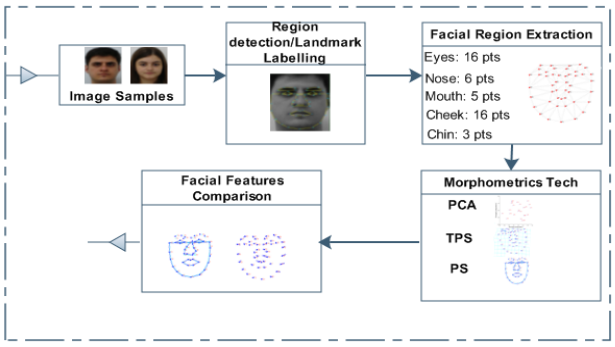

Fig. 1: Gender Comparison Architecture

3. Materials & Methods

3.1. Data Description

Different facial databases perform better in different research application areas such as face recognition, facial expression recognition etc.; some are two-dimensional while some are three-dimensional. This research uses FEI face dataset which was captured in Brazil at Artificial Intelligent Lab. The research uses a total of 50 images consisting of 25 males and 25 females between the age of 19 and 40 years. The dataset is used due to its two-dimensionality, age-group and it has achieved a greater performance on gender-based comparison over the years [8]. This small sample is used to test the performance of the method and work within the timeframe, larger sample size will be used in the feature research with other datasets comparison.



Fig. 2: FEI dataset: male (top), female (bottom)

3.2. Facial Landmark and Features Extraction

The experiment contains 50 faces manually landmarked (25 male and 25 female) with 46 homologous landmarks. The landmark is categorized into two segments: male face (MF) and female face (FF). Figure 3 shows the 46 landmarks with selected features. We will not be able to describe all the facial features in the face here for lack of space but the majorly selected anatomical regions are the eyes, nose, mouth, cheek and chin as shown in Table 1.

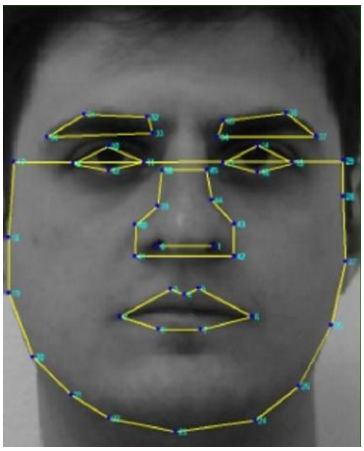

Fig. 3: 46 annotated facial landmark with selected features

Table 1: Selected Facial Features with Landmarks

Facial Regions	Selected Features	Landmarks
Eyes	Eyebrow	31-32-33-34, 35-36-37-38
	Eyeball	10-11-12-13, 14-15-16-17
Nose	Nose width (upper)	39-46
	Nose width (lower)	42-43
Mouth	Mouth width	3-7
Chin	Chin drop	23-24, 24-25
Cheek	Cheek width	21-27, 20-28

3.3. Principal Component Analysis

The concept of PCA is finding a low-dimension set of axes that summarize data. Mathematically, linear transformation is performed by PCA by moving the original set of features composed of the principal component to a new space [9].
The method uses the concepts of covariance matrix, variance matrix, eigenvalues and eigenvector pairs to perform PCA, providing a set of eigenvectors and its respective eigenvalues as a result. The PCA algorithm computes the covariance matrix of the images with its eigenvalues and eigenvectors coupled with the components that correspond to the top few largest eigenvalues are retained to reduce dimension [10].
PCA first computes the sample covariance matrix using:

$$\hat{E} = \frac{1}{n}\sum_{i=1}^{n}(X_{\mathrm{i}} - \bar{X}_n)\,(X_{\mathrm{i}} - \bar{X}_n)^{\mathrm{T}} \tag{1}$$

Then the eigenvalues $\lambda 1 \geq \lambda 2 \geq \ldots$ is computed with eigenvectors e1, e2… of covariance matrix $\hat{E}$, while choosing a dimension k, we define the dimension reduced data to:

$$Z_i = T_k(X_i) = \sum_{j=1}^{k} \beta_{\mathrm{ij}} \mathrm{e_j} \tag{2}$$

Where

$$\beta_{\mathrm{ij}} \mathrm{e_j} = \left(X_{\mathrm{i}} - \bar{X},\ e_j\ \right) \tag{3}$$

In this research, the variances and eigenvalues were computed on the 24 PCs of each group, though not shown for lack of space. Figures 6-10 show the results of the PCs and the variances.

3.4. TPS Warping

The techniques behind TPS is choosing two sets of coordinate information in two images that are corresponding from different or same imaging methods to mapping the information of the pixel obtained from image A to another image B of same correspondence. TPS can always match the corresponding coordinate information exactly, and keep the entire image deforming energy in minimum [11]. The research defines array information of two sets of coordinate as P_i and h_i for each sex group (Male: A and Female: B). The $P_i = (x_i, y_i)$ and $h_i = (X_i, Y_i)$ are the points of control belonging to the face image A and face image B, respectively. The mapping transformation Φ, mapping the coordinate point from face image A to the face image B based on the Equation (4), can be determined after the computational matching. The numbers of the matching points selected shown in Equation (4) determines the coefficient mapping transformation

$$\Phi(P) = a_1 + a_{1x}\mathrm{x} + a_y\mathrm{y} + \sum_{i=1}^{n} \omega_1 \mathrm{U}(|\mathrm{P} - \mathrm{P_i}|) \quad (4)$$

where P = (x, y) denotes coordinates of the face space. In the determination of the coefficients in Equation (1), the operation of the matrix W is estimated and formed as (n+3) × 2, defined as:

$$W = (\omega \ldots \omega_n \, a_1 \, a_x \, a_y)^T = L^{-1}\mathrm{M} \quad (5)$$

where the $\omega_1, \omega_2, \ldots, \omega_n$; a_1, ax, and a_y are the primary coefficients of the TPS. As shown in Equation (5), W and L represent the matrixes and the M matrix is computed as (n+3) ×2,

$$M = (h_1 \, h_2 \, \ldots \, h_n \, 0 \, 0 \, 0)^T \quad (6)$$

where $h_i = (X_i, Y_i)$, and I = 1, …, n, which is the control points of selected coordinates in plane B, forming L matrix as (n+3) × (n+3) with the merging of matrix Q, matrix K, and another zero matrixes with (3 × 3),

$$L = \begin{bmatrix} K & Q \\ Q^T & O \end{bmatrix} \quad (7)$$

Operation Q and K are defined in order to determine L, such that K is:

$$K = \begin{bmatrix} 0 & U_{12} & \cdots & U_{1n} \\ U_{21} & 0 & \cdots & U_{2n} \\ \vdots & \vdots & \ddots & \vdots \\ U_{n1} & U_{n2} & \cdots & 0 \end{bmatrix} \quad (8)$$

Where $U(r) = r^2 \log r$ and $r_{ij} = |P_i - P_j|$ is the length of two arbitrary two selected control points in image A, defining Q as:

$$Q = \begin{bmatrix} 1 & x_1 & y_1 \\ 1 & x_2 & y_2 \\ \vdots & \vdots & \vdots \\ 1 & x_n & y_n \end{bmatrix} \quad (9)$$

where (x_i, y_i), I = 1, …, n, is denoted as image A control point coordinate. Estimating the coefficients ($w_1, w_2, \ldots, w_n$; a_1, a_x, and a_y) by the Equation (5) will help achieve TPS mapping function between the corresponding points in image A and B. The corresponding coordinate point in image B is obtained when there is a substitution of two arbitrary points given as ($|P\text{-}P_i|$) in image A and a coordinate of arbitrary point P (x, y) into Equation (4).
Based on the appearance of the object in Figure 4, this research propose a direct technique for estimating the TPS warp between the two sets of the image group.

3.5. Procrustes superimposition

Procrustes fitting of face images involves translation, scaling and rotation of all the faces such that the aggregate distances between corresponding landmarks in the least squares is as small as possible [12]. In order to have the same centroid size, the landmark configuration is scaled which is a measure of scale for landmark configurations [13, 14]. One of the two centered scaled configuration is rotated around its centroid until the sum of the squared during superimposition of landmark configuration [15].

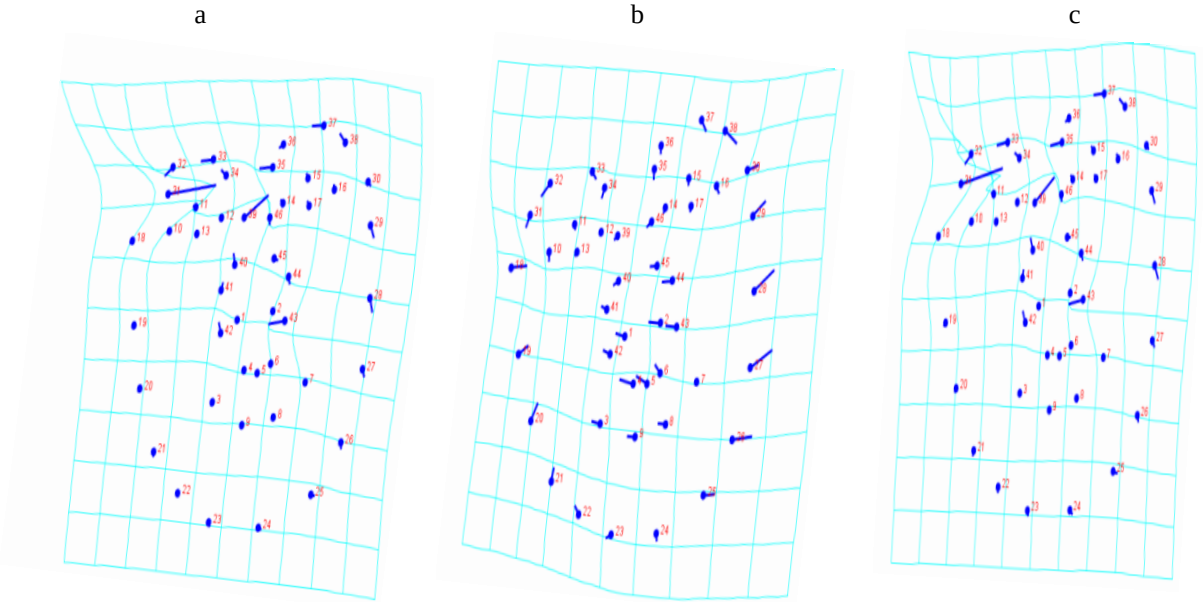

Fig. 4: (a) TPS for male group, (b) TPS for female group, (c) combined TPS fitting for male and female

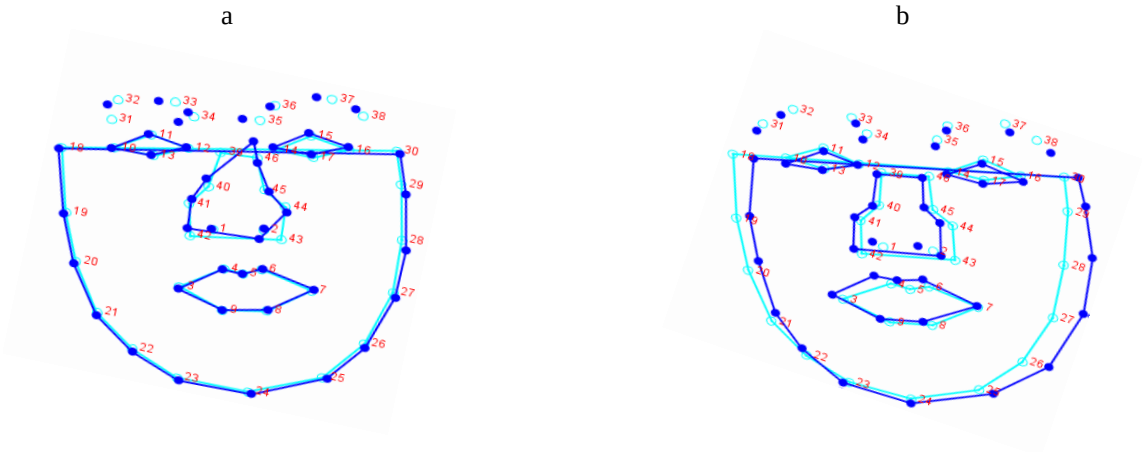

Fig. 5: Procrustes fittings for (a) male, (b) female respectively

In 2D, the Procrustes fitting is easily relatively computed such that if X_1 and X_2 are k x p matrices where p=2 or 3, for the coordinates of k landmarks after rescaling and centering. If the decomposition of singular value of $X_1^t X_2$ is UDV^t with the element of D positive, then to superimpose X_2 upon X_1 optimally, the rotation needed is the matrix VU^t, for 3x3 or 2x2. For the two complex vectors $z_j = (z_{1j}\ldots, z_{kj})^t$, j = 1, 2, with $\sum_i zij = 0$ and $\sum_i z_{ij}\,\bar{z}_{ij} = 1$, in a different notation, the superimposition of the second form upon the first is approximately:

$$z_2 \rightarrow \left(\sum_i z_{i1}\bar{z}_{i2}\right) z_2 \qquad (10)$$

Then between the two sets face group, the Procrustes distance is approximately:

$$PD^2\,(Z_1, Z_2) = 1 - \left|\sum_i z_{i1}\bar{z}_{i2}\right| \qquad (11)$$

The application of Procrustes was employed to the fittings of male and female group facial landmarks with translation, scaling and rotation to achieve the two objects as shown in Figure 5, though it is crystal clear that the male landmark is more fitting than that of female.

4. Results & Discussions

4.1. PCA Variation

The analysis of the result is carried out in morphoj, a morphometrics analysis package developed by Klingenberg lab in Manchester University. The PCA tells which differences in the shape are responsible for the variation. The chart breaks the shapes into Principal Components (PC), where PC1 shows the most variation; PC2 shows the next biggest, and so on. Here, the total variable for male and female faces is 24, though only 20 showing as the rest is fading out. The first PC shows a greater variation of more than 77% for male while the first four PCs show more than 67% variation for female. The total variation shown by the first four PCs of female faces is lesser than the variation shown by the first PC of male faces. Figure 6 and Figure 7 show the PCs and the percentage change in the variances for male and female faces respectively.

Looking at how male and female faces plot out on PC1 and PC2, this graph is often referred to as morphospace in morphometrics, though always called scatter plot. If two faces are closed on the graph, they are similar in shape and in morphospace. If a category, e.g. male or female has a big spread, then they have a wide distribution in morphospace. Figure 8 and Figure 9 show the distribution of the male and female faces in morphospace respectively, while Figure 10 shows a categorized distribution of both male and female faces in morphospace. Though, the spread in Figure 8 is much closer or has a lower distribution at the centre of x, y axis except faces m1a, m3a and m44a. Along PC1, m3a and m44a spread to positive axis while along PC2, m1a spreads towards positive axis which indicates that m1a, m3a and m44a have significant face shape different from other male groups. In figure 9, along with the PC1, f87a and f98a are overlapping along the positive axis, though there is wider spread in the female group. But the overlapping of f87a and f98a shows that they both have similar face shape in the morphospace. In figure 10, there is a lower spread between the sex groups but there still a repeating of wider spread of m1a, m3a and m44a in the morphospace.

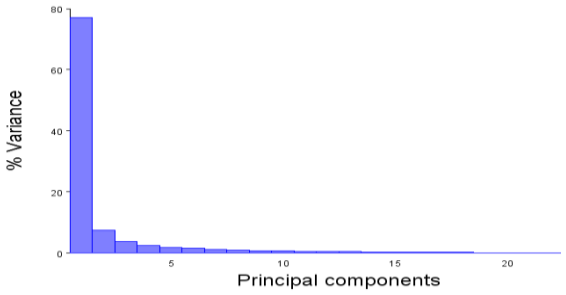

Fig. 6: Percentage variance change of PCs for male faces

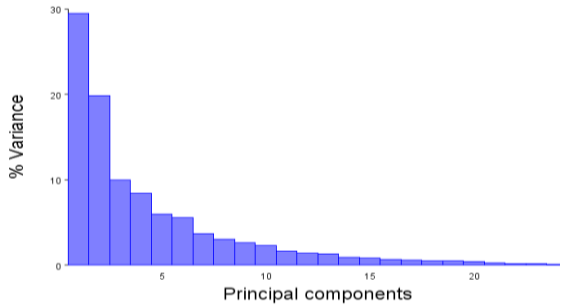

Fig. 7: Percentage variance change of PCs for female faces

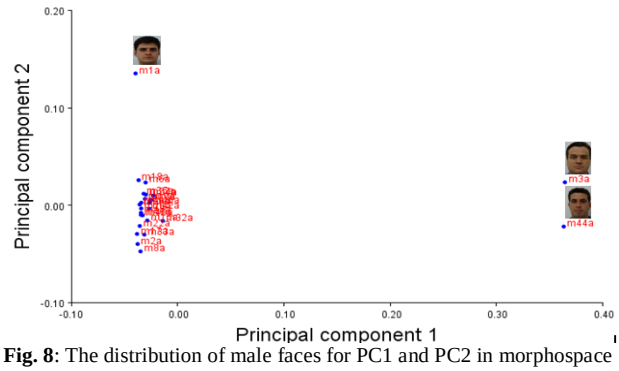

Fig. 8: The distribution of male faces for PC1 and PC2 in morphospace

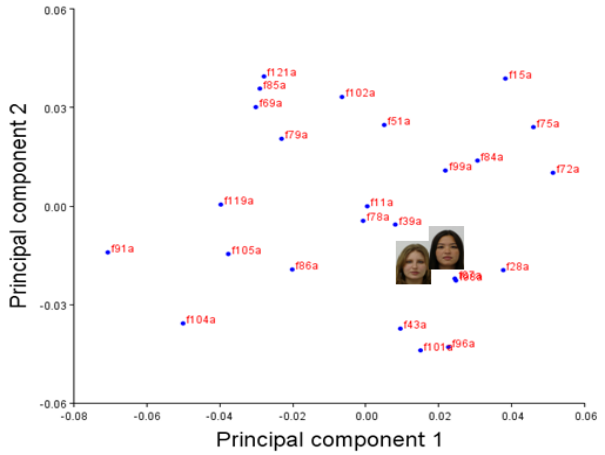

Fig. 9: The distribution of female faces for PC1 and PC2 in morphospace

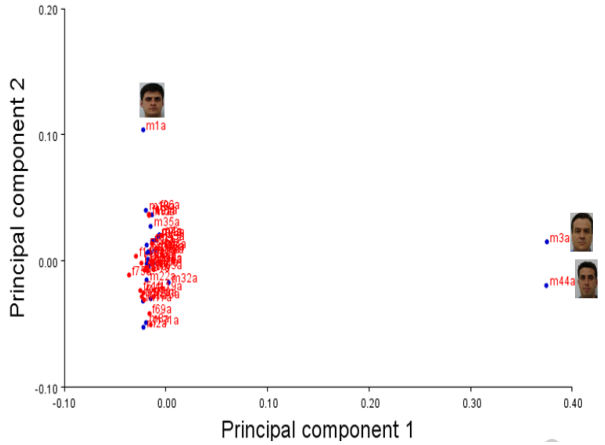

Fig. 10: The distribution of male and female faces for PC1 and PC2 in morphospace

4.2. Facial Features Comparison

In the lollipop graph for male and female generated from TPS (Figure 11), each of those blue circles is the average position of the landmarks we selected. The length of the sticks tells us which way things change along the principal components. In the male group, the eyebrows are longer than that of the female group; also the eyeballs in the male group are bigger compared to the female group. Female nose is wider but the male nose is longer, the female group has a wider mouth (with lips) than the male group; the female group cheek is more round and wider than the male group. It is also discovered that the female group has a little more chin drop than the male group. The comparison of the work with other relsted work (Table 2) indicates that the method is completely race dependent rather than machine dependent.

Table 2: Facial Features Results Compared

Author	Method	Dataset	Reports
Koudelová, et al. [3]	DCA + PCA	White Caucasian adult	The reports concluded that generally, males had more prominent deeply set eyes, eyebrow ridges, flatter cheek area, and a more prominent chin area and nose than female
This work	PCA+TPS+PS	FEI (Brazilian)	Generally, male has wider eyebrows, bigger eyeballs and longer nose; female has wider nose, wider mouth, wider and rounded cheek and chin drop

5. Conclusion

There has been a substantial improvement in the capabilities of sexual facial comparison as a result of on-going studies on geometric morphometrics. However, many challenging problems related to the presentation and interpretation of facial feature to non-experts in computer vision. In this context, this work proposes handful sets of facial features for sexual facial comparison which has been described and metrically evaluated. Hence, gender differences in the facial morphology of the sample were studied by means of morphometrics techniques. Due to the direct observable differences and its superiority to the conventional metric method that analyses angles, ratio and distance separately, this procedure proves to be one of the most interesting techniques proposed for the analysis of biological gender-based form differences [16]. Also, its application and interpretation are easier than those of finite element analysis by taken the whole structure into account at a time [17].

Here, the major and easily observable facial landmark features are extracted in the regions of eyes, nose, mouth, cheek and chin; PCA is performed to find low-dimensional sets of an axis that summarize data, the algorithm uses the concept of the variance matrix, covariance matrix, eigenvalues and eigenvectors to perform PCA, though the PCA could not give us much clear result on the gender comparison when the groups are combined in the morphospace. TPS warping was also applied to align and match the faces, with Procrustes fittings to eliminate the non-shape component of variation based on size, position and orientation.

The results show percentage variance and landmark distribution in the morphospace where some faces are observed to be widely spread (m1a, m3a, m44a) in male and some overlapping of faces (f87a and f98a) in the female. Furthermore, the facial features for gender significant using TPS and PS in Figure 5 and Figure 11 respectively are compared, and many facial features are found to be dissimilar between the two gender groups such as wider eyebrows, bigger eyeballs and longer nose for male group; and wider nose, wider mouth, wider and rounded cheek and chin drop for female group, the test achieved a p-value of 0.0071 ($p < 0.5$). The results of the analysis show that the research is scientifically significant and there is significant gender difference between the male and female sex groups considering selected facial features this method serves as alternative method for gender-based facial features comparison.

Acknowledgement

This research is supported by Fundamental Research Grant Scheme.

References

[1] C. Tanikawa, E. Zere, and K. Takada, "Sexual dimorphism in the facial morphology of adult humans: a three-dimensional analysis," *HOMO-Journal of Comparative Human Biology*, vol. 67, pp. 23-49, 2016.

[2] H. Matthews, T. Penington, I. Saey, J. Halliday, E. Muggli, and P. Claes, "Spatially dense morphometrics of craniofacial sexual dimorphism in 1-year-olds," *Journal of anatomy*, vol. 229, pp. 549-559, 2016.

[3] J. Koudelová, J. Brůžek, V. Cagáňová, V. Krajíček, and J. Velemínská, "Development of facial sexual dimorphism in children aged between 12 and 15 years: a three-dimensional longitudinal study," *Orthodontics & craniofacial research*, vol. 18, pp. 175-184, 2015.

[4] V. F. Ferrario, C. Sforza, G. Pizzini, G. Vogel, and A. Miani, "Sexual dimorphism in the human face assessed by euclidean distance matrix analysis," *Journal of Anatomy*, vol. 183, p. 593, 1993.

[5] C. DeLacoste-Utamsing and R. L. Holloway, "Sexual dimorphism in the human corpus callosum," *Science*, vol. 216, pp. 1431-1432, 1982.
[6] A. C. Little, B. C. Jones, C. Waitt, B. P. Tiddeman, D. R. Feinberg, D. I. Perrett, *et al.*, "Symmetry is related to sexual dimorphism in faces: data across culture and species," *PloS one*, vol. 3, p. e2106, 2008.
[7] I. M. Scott, A. P. Clark, S. C. Josephson, A. H. Boyette, I. C. Cuthill, R. L. Fried, *et al.*, "Human preferences for sexually dimorphic faces may be evolutionarily novel," *Proceedings of the National Academy of Sciences*, vol. 111, pp. 14388-14393, 2014.
[8] C. E. Thomaz and G. A. Giraldi, "A new ranking method for principal components analysis and its application to face image analysis," *Image and Vision Computing*, vol. 28, pp. 902-913, 2010.
[9] M. E. Wall, A. Rechtsteiner, and L. M. Rocha, "Singular value decomposition and principal component analysis," in *A practical approach to microarray data analysis*, ed: Springer, 2003, pp. 91-109.
[10] N. D. Jaglan, "A Literature Review: Various Facial Expression," *Journal of Network Communications and Emerging Technologies (JNCET) www. jncet. org*, vol. 7, 2017.
[11] Y.-C. T. H.-D. Lin, Y.-C. H. C.-L. Yu, and K.-P. Lin, "Thin-plate spline technique for medical image deformation," *Journal of medical and biological engineering*, vol. 20, pp. 203-210, 2000.
[12] P. O'Higgins and I. Dryden, "Studies of craniofacial development and evolution," *Archaeology in Oceania*, vol. 27, pp. 105-112, 1992.
[13] F. L. Bookstein, "Landmark methods for forms without landmarks-morphometrics of group differences in outline shape," *Medical Image Analysis*, vol. 1, 1997.
[14] I. L. Dryden and K. V. Mardia, *Statistical Shape Analysis* vol. 4. Chichester: Wiley, 1998.
[15] F. J. Rohlf, "Relative warp analysis and an example of its application to mosquito," *Contributions to morphometrics*, vol. 8, p. 131, 1993.
[16] F. L. Bookstein, "A statistical method for biological shape comparisons," *Journal of Theoretical Biology*, vol. 107, pp. 475-520, 1984.
[17] P. E. Lestrel, "Some approaches toward the mathematical modeling of the craniofacial complex," *J Craniofac Genet Dev Biol*, vol. 9, pp. 77-91, 1989.

a b

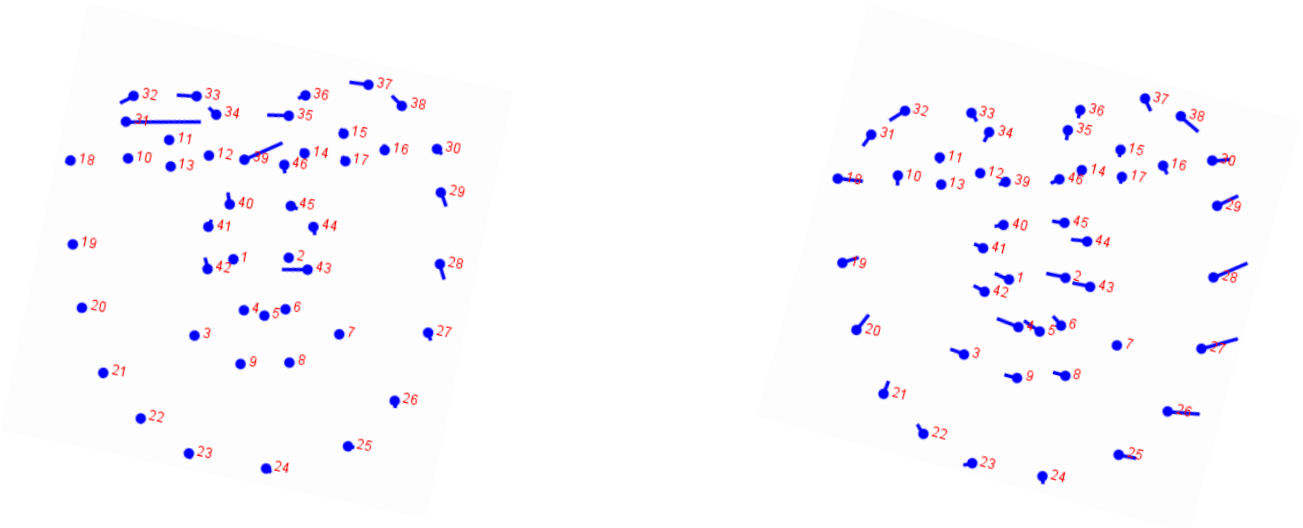

Fig. 11: Lollipop graph from TPS for (a) male, (b) female respectively